AFM-IN-SEM ANALYSIS ON HETEROSTRUCTURE EDGES OF GRAPHENE AND HEXAGONAL BORON NITRIDE

[1*]Jaroslav KULIČEK, [2]Takatoshi YAMADA, [3]Takashi TANIGUCHI, [1]Bohuslav REZEK

[1]*Faculty of Electrical Engineering, Czech Technical University in Prague, Prague, Czech Republic, EU*,
kulicjar@fel.cvut.cz
[2]*National Institute of Advanced Industrial Science and Technology, Tsukuba, Japan*
[3]*National Institute for Material Science, Tsukuba, Japan*

Abstract

Correlative microscopy methods have become significant due to the possibility of examining several material properties during one measurement. Atomic Force Microscopy in Scanning Electron Microscopy (AFM-in-SEM) is a correlative method that allows the simultaneous detection and acquisition of signals from both methods. Heterostructures of Graphene and hexagonal Boron Nitride (G/hBN) are studied with view to many electronic applications due to the possibility of tuning their electronic properties. In this work, we study electronic properties at the edges of single layer G on hBN flakes of various thicknesses prepared on Si and SiO_2 substrates. Electronic properties are studied by AFM-in-SEM correlative microscopy that provides simultaneous acquisition of signals from both methods. Images of G/hBN heterostructure flakes obtained in the secondary electron detector show an enhanced signal along the edges that is attributed to localized electrons. We discuss how it corroborates a model that enhanced Raman signal of 2D and Si peaks on the G/hBN edges is electronic (plasmonic) rather than an optical or structural effect.

Keywords: AFM-in-SEM, correlative microscopy, graphene, boron nitride, electronic properties

1. INTRODUCTION

Graphene/hBN heterostructures are studied in electronic applications due to tuning electronic possibilities, such as self-powered photodetectors and sensing and biosensing applications [1–3]. G/hBN heterostructures on Si substrates have been used in self-powered photodetectors, where a thin hBN film was the carrier transport material, which averted interlayer coupling at the interface [1]. The study of graphene plasmons has been in focus for many years, and the plasmonic effect has also been studied on G/hBN heterostructures [4–6]. Plasmonic effects were primarily observed under infrared (IR) illumination [7,8]. Vincent *et al.* [8] studied bubbles in closely spaced networks in G/hBN heterostructures and showed an enhancement of IR absorption. This observation was attributed to surface plasmon polaritons. Recently, a work was published where graphene plasmons were observed in visible light on heavily nano-corrugated layers of mechanically exfoliated graphene flakes on SiO_2/Si substrates [9]. Interestingly, research on G/hBN electrical properties including graphene plasmons has mainly focused on the flake surface whereas research on electrical properties on G/hBN edges is negligible although they may in principle impact various electronic properties. We have reported effect of visible Raman enhancement at the edge [10], however, the suggested plasmonic model needs further exploration.

Recently, correlative microscopy, combining two or more independent microscopy techniques, has taken an important place in material research due to the possibility of studying several properties simultaneously in the same location, parameters and environment. Atomic force microscopy in scanning electron microscopy (AFM-in-SEM) enables measurement of materials in vacuum and the same place, providing information about the

studied materials structural and electrical properties. Thus, the morphology and structure of the SEM overlap to form a Correlation Probe Electron Probe (CPEM) image. Dinarelli *et al.* [11] used the AFM-in-SEM method to study workflows on calcite moonmilk, a calcium carbonate extracted from ancient tombs. In another work, Rutherford et al. [12] studied AFM-in-SEM bacteria-metal nanocomposite and, due to CPEM images, could recognize the position of silver and diamond nanoparticles on/under bacteria.

In this work, we employ the CPEM method to study G/hBN heterostructure edges on Si substrate. Heterostructures were prepared using high-pressure high-temperature (HPHT) hexagonal boron nitride flakes on SiO_2 or Si substrates overlaid with chemical vapor deposition (CVD) single-layer graphene. Structural and electronic properties were analyzed by AFM-in-SEM and correlated also with Raman micro-spectroscopy and Kelvin probe force microscopy (KPFM). We observe an enhancement of the SEM signal on the G/hBN edges and high steps related with enhanced Raman signal in visible light range.

2. MATERIAL AND METHODS

High-pressure high-temperature hexagonal boron nitride was prepared by the standard method described in. Flakes were transferred on SiO_2/p-Si substrates or p-Si substrates by mechanical exfoliation. Single layered graphene was prepared by chemical vapor deposition (CVD) on copper foil. Subsequently, graphene was transferred and laid over the substrate with hBN flakes. The PMMA transfer method was used for the deposition of graphene on the substrate [13].

Graphene/hBN flakes were analyzed by Raman spectral mapping. The WITec alpha 300 RAS system was used to record Raman spectral maps in reflection mode using an integrated spectrometer (grating G2 with 600 grooves/mm, CCD detector) and a 532 nm fiber-coupled laser for excitation. Raman spectral maps were recorded for a 25 x 25 μm^2 area, scan speed 7.612 s/line, 150x150 pixels per image.

Contact potential difference (CPD) measurement in Kelvin probe force microscopy (KPFM) mode was also performed at the WITec system. The samples were grounded with a spring contact from the top on graphene. The CPD maps of G/hBN heterostructures were obtained in the dark. Two-pass amplitude-modulated mode (AM) KPFM regime with the Multi75E cantilevers was used for optimal measurements. The scan parameters were: area 50 × 50 μm^2, set point 0.6 V, scan speed 2.56 s/line, 256 × 256 pixels per image. The a.c. driving voltage amplitude 3.0 V (6.0 V_{pp} peak-to-peak) and the height offset 30 nm were used in the 2nd pass.

Atomic Force Microscopy (AFM) measurements were performed using the LiteScope 2.0 system using Akiyama cantilevers with a 5 N/m nominal stiffness. The scanning area was 70 x 70 μm^2, 512 x 512 pixels, images were collected with a scanning speed of 10 μm/s, CI = 0.065, CP = 0.2 and setpoint 13 Hz.

The morphology of G/hBN flakes was obtained by a Zeiss EVO 10 Scanning Electron Microscope (SEM). The SEM images of G/hBN flakes were acquired at acceleration voltage (EHT) 1-5 kV and a magnification of 2.5 kX in the SE regime using an off-beam detector and BSE detector. WD was 11.86 mm and I Probe 5 pA.

Alignment of simultaneously obtained AFM and SEM images and CPEM correlation analysis was performed using softwares NenoView and Gwyddion version 2.63 [14].

3. RESULTS AND DISCCUSION

The optical image, contact potential map, Raman map in Si peak and 2D peak of G/hBN are shown in **Figure 1**. In the optical image, the flake is well visible with pronounced dark edges (**Figure 1a**). In the CPD map (**Figure 1b**) the potential is generally uniform, some variations (visibility enhanced by adjusting the color z-scale to 25 mV) are most likely caused by wrinkles and bubbles that arose during the deposition of graphene on the substrate. There is also a distinct feature on the flake though: the dark boundaries within the G/hBN flake and along some part of its edge. As the graphene is laid all over the structure, the dark contrast corresponds to negative charge (electrons) localized at these features. **Figure 1c** shows the Raman map of

Si peak intensity on the G/hBN flake. The Raman map is well correlated with the optical image, various domains are visible. In addition, at certain places and edges, the signal intensity is significant, corresponding to a bright yellow color. The signal enhancement is also visible at the edges of the G/hBN flake in the Raman map of 2D graphene peak (**Figure 1d**). The enhancement at the edge could be caused by the localization of electrons, i.e. by localized plasmonic vibrations under visible light illumination, as we suggested in our prior work [10]. Note that we did not observe a similar effect on G/hBN heterostructures on the SiO₂ substrate, thus it cannot not be merely structural effect or optical effect. The question arose whether the same effect would be observed in SEM, where interaction with electrons in the sample is detected.
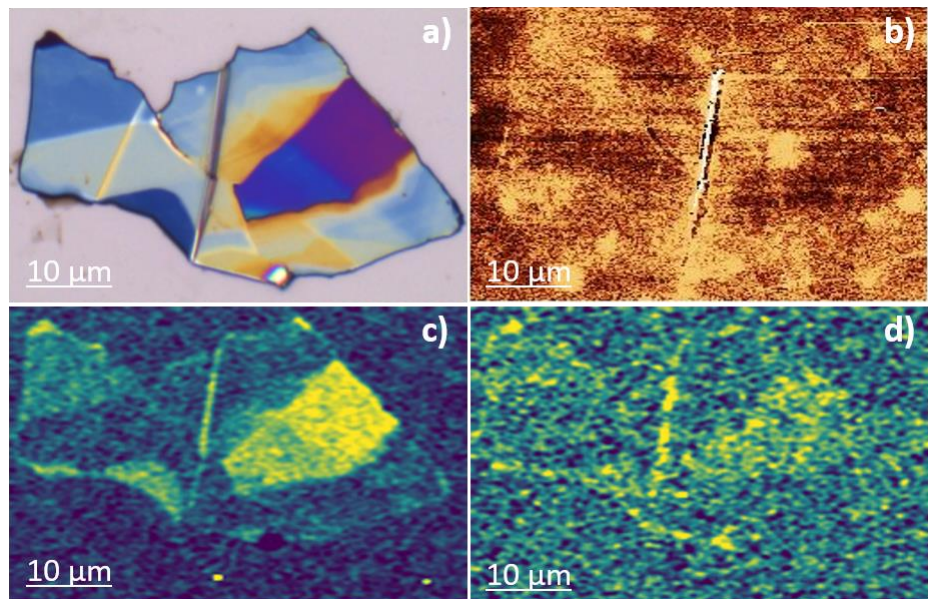
Figure 1 Images of G/hBN flake on Si substrate **a)** optical, **b)** contact potential difference map, (color scale 25 mV), Raman map of **c)** Si peak and **d)** 2D peak intensity.

Figure 2 shows G/hBN flake SEM images in SE mode under different acceleration voltages 1 kV - 5 kV to probe electronic effects in the G/hBN structure by using electrons of different energy, i.e. with different depth and material penetration. Generally, we can recognize some bright edges and boundaries within the flake in all the SEM images, although with different intensity and clarity. At acceleration voltage 5 kV, also some gray domains are visible, which are similar also on surrounding substrate. As the bare silicon substrate is featureless in SEM, they must thus correspond to domains in graphene that is laid all over the substrate and the flake. They become visible by shining through the graphene with high energy primary electrons and secondary electrons, as indicated in prior work [15]. These features diminish with decreasing acceleration voltage. At the low acceleration voltage 1 kV the image is overall uniformly grey with features resembling the KPFM potential map in **Figure 1b**. This indicates that we see mostly
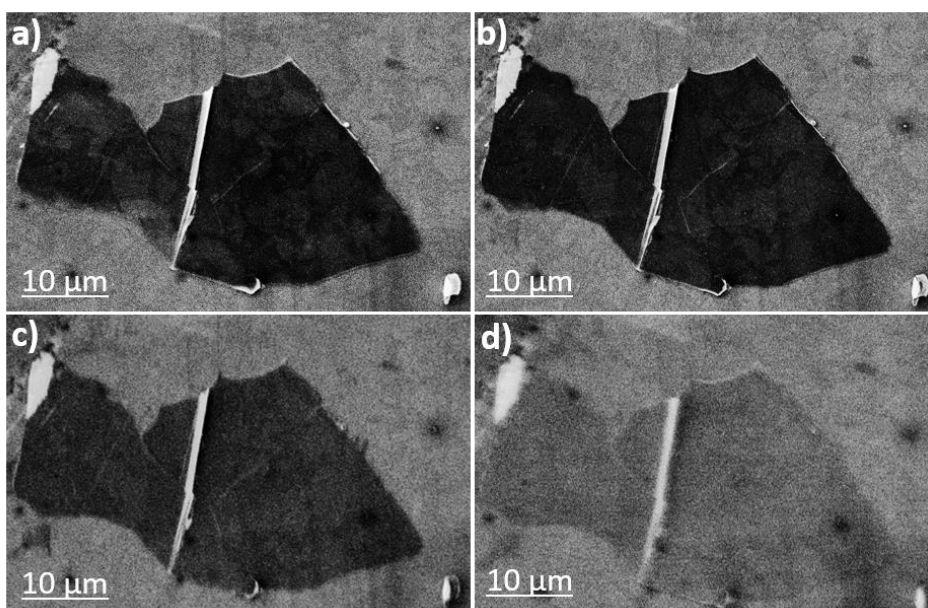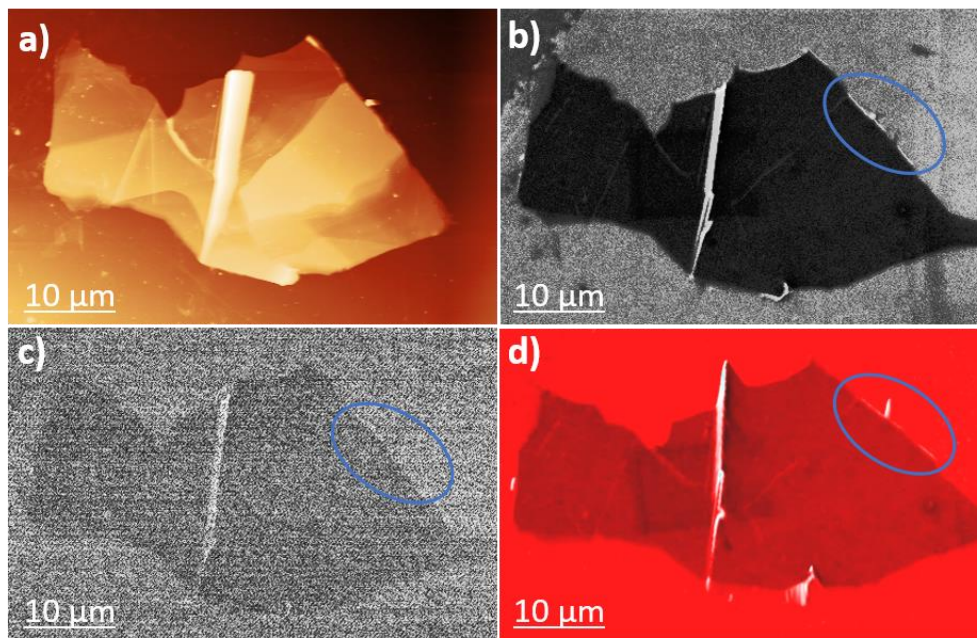

Figure 2 SEM images of G/hBN flake on Si substrate at different accelerating voltage **a)** 5 kV, **b)** 3 kV, **c)** 1.5 kV and **d)** 1 kV.

electronic properties of graphene on top of the hBN and Si substrate. Yet the brighter edges and boundaries remain recognizable. Thus they are most likely related with the localized electrons. The enhancement of the SEM signal at the edges of the G/hBN flake supports our previous results about the electrical effect at the flake edges observed in the Raman maps.

In order to directly correlate the topographical structure with electronic contrast we performed the CPEM analysis by correlative AFM-in-SEM measurements. We employed acceleration voltage 3 kV as it showed the best contrast between the substrate, the flake and the signal enhancement at the edges. The results are shown in **Figure 3**: a) AFM surface height morphology, b) SEM image of secondary electrons, c) SEM image of backscattered electron detector, and d) combined three-dimensional CPEM image. G/hBN morphology shows regions of various height on the flake, some smooth and some more structurally pronounced edges such as in the middle of flake (height 400 nm). AFM morphology is well correlated with Raman and SEM images. The edge in the middle of flake is visible in both SE and BSE detector SEM images. In addition, the SEM images show an enhanced signal at the edge between the substrate and the flake (blue circle in **Figures 3 b** and **3c**). An enhanced signal at the edge between the substrate and the flake is seen for both SE and BSE detectors.

Figure 3 G/hBN flake on Si substrate **a)** AFM surface height morphology, **b)** image of secondary electrons (acceleration voltage 3 kV), **c)** image of backscattered electrons (acceleration voltage 3 kV), and **d)** combined 3D CPEM image.

Furthermore, the overlay of AFM and SEM SE mode images was done to verify whether the enhancement of the SEM signal on the G/hBN edge is due to a structural or electronic effect. **Figure 3d** shows a CPEM image in 3D where white represents the enhancement of signal. One particular area at the G/hBN edge is marked by a blue circle. The flake edge is white there while the morphology is flat. The enhancement of the SEM signal is visible in the CPEM image also at other parts of the flake edge as well as at some height boundaries within the flake. This all confirms that the enhancement of signal is the electronic effect.

4.   CONCLUSION

In conclusion, the electron accumulation at the G/hBN heterostructures edge was studied by correlative microscopy using AFM-in-SEM with Raman and KPFM. Raman maps indicated the effect via an enhanced signal on the G/hBN flake surface and partially on the edges between Si substrate and flake in Si and 2D

peaks. The most enhanced regions were also indicated by negative potential features in the KPFM image. SEM images showed corresponding enhancement of the secondary as well as back scattered electron signal. The combined CPEM image confirmed the electronic effect, i.e. visible frequency plasmons, behind the Raman enhancement. The edge of G/hBN heterostructure has thus potential in sensing applications.

ACKNOWLEDGEMENTS

REFERENCES

[1]   WON, U. Y.; LEE, B. H.; KIM, Y. R.; KANG, W. T.; LEE, I.; KIM, J. E.; LEE, Y. H. and YU, W. J. Efficient photovoltaic effect in graphene/h-BN/silicon heterostructure self-powered photodetector. *Nano Res.* 2021, vol. 14, pp. 1967–72.

[2]   LIU, Z.; LU, F.; JIANG, L.; LIN, W. and ZHENG, Z. Tunable Goos-Hänchen Shift Surface Plasmon Resonance Sensor Based on Graphene-hBN Heterostructure. *Biosensors.* 2021, vol. 11, 201.

[3]   SHUKLA, V.; JENA, N. K.; GRIGORIEV, A. and AHUJA, R. Prospects of Graphene–hBN Heterostructure Nanogap for DNA Sequencing. *ACS Appl. Mater. Interfaces.* 2017, vol. 9, pp. 39945–52.

[4]   TIZEI, L. H. G.; LOURENÇO-MARTINS, H.; DAS, P.; WOO, S. Y.; SCARABELLI, L.; HANSKE, C.; LIZ-MARZÁN, L. M.; WATANABE, K.; TANIGUCHI, T. and KOCIAK, M. Monolayer and thin h–BN as substrates for electron spectro-microscopy analysis of plasmonic nanoparticles. *Appl. Phys. Lett.* 2018, vol. 113, 231108.

[5]   ZHANG, K.; YAP, F. L.; LI, K.; NG, C. T.; LI, L. J. and LOH, K. P. Large Scale Graphene/Hexagonal Boron Nitride Heterostructure for Tunable Plasmonics. *Advanced Functional Materials.* 2014, vol. 24, pp. 731–8.

[6]   ZHANG, Z., LEE, Y., HAQUE, M. F., LEEM, J., HSIEH, E. Y. and NAM, S. Plasmonic sensors based on graphene and graphene hybrid materials. *Nano Convergence.* 2022, vol. 9, vol. 28.

[7]   FEI, Z., FOLEY, J. J., GANNETT, W., LIU, M. K., DAI, S., NI, G. X., ZETTL, A., FOGLER, M. M., WIEDERRECHT, G. P., GRAY, S. K. and BASOV, D. N. Ultraconfined Plasmonic Hotspots Inside Graphene Nanobubbles. *Nano Letters.* 2016, vol. 16, pp. 7842–8.

[8]   VINCENT, T., HAMER, M., GRIGORIEVA, I., ANTONOV, V., TZALENCHUK, A. and KAZAKOVA, O. Strongly Absorbing Nanoscale Infrared Domains within Strained Bubbles at hBN–Graphene Interfaces. *ACS Appl. Mater. Interfaces.* 2020, vol. 12, pp. 57638–48.

[9]   DOBRIK, G.; NEMES-INCZE, P.; MAJÉRUS, B.; SÜLE, P.; VANCSÓ, P.; PISZTER, G.; MENYHÁRD, M.; KALAS, B.; PETRIK, P.; HENRARD, L. and TAPASZTÓ, L. Large-area nanoengineering of graphene corrugations for visible-frequency graphene plasmons. *Nat. Nanotechnol.* 2022, vol. 17, pp. 61–6.

[10] KULIČEK, J., YAMADA, T., TANIGUCHI, T. and REZEK, B. Visible-frequency plasmonic enhancement at the edge of graphene/h-BN heterostructures on silicon substrate. *Carbon.* 2024, 118836.

[11] DINARELLI, S., MURA, F., MANCINI, C., PENNA, G. L., RINALDI, T. and ROSSI, M. (2022). Comparison of different correlative AFM-SEM workflows on calcite moonmilk. *IOP Conf. Ser.: Mater. Sci. Eng.* 2022, vol. 1265, 012011.

[12] RUTHERFORD, D., KOLÁŘOVÁ, K., ČECH, J., HAUŠILD, P., KULIČEK, J., UKRAINTSEV, E., STEHLÍK, Š., DAO, R., NEUMAN, J. and REZEK, B. Correlative atomic force microscopy and scanning electron microscopy of bacteria-diamond-metal nanocomposites. *Ultramicroscopy.* 2024, vol. 258, 113909.

[13] YAMADA, T., MASUZAWA, T., EBISUDANI, T., OKANO, K. and TANIGUCHI, T. Field emission characteristics from graphene on hexagonal boron nitride. *Appl. Phys. Lett.* 2014, vol. 104, 221603.

[14] NEČAS, D. AND KLAPETEK, P. Gwyddion: an open-source software for SPM data analysis. *Open Physics* 2012, vol. 10, pp. 181–8.

[15] SHIHOMMATSU, K., TAKAHASHI, J., MOMIUCHI, Y., HOSHI, Y., KATO, H. and HOMMA, Y. (2017). Formation Mechanism of Secondary Electron Contrast of Graphene Layers on a Metal Substrate. *ACS Omega. 2017, vol.* 2, pp. 7831–6.